Proceedings of the 4th African Rift Geothermal Conference
Nairobi, Kenya, 21-23 November 2012

Petrogenesis of the Suswa Volcano, Kenya

John Charles White, Vanessa V. Espejel-García, Elizabeth Y. Anthony, and Peter A. Omenda

Eastern Kentucky University, USA; University of Texas at El Paso, USA; Geothermal Development Company, Kenya

john.white@eku.edu; vanessa_espejel@yahoo.com; eanthony@utep.edu; pomenda@gdc.co.ke

Keywords: Trachyte, Phonolite, Central Kenya Peralkaline Province

ABSTRACT

Mount Suswa is a large (>700 km^2) trachytic shield volcano with two nested summit calderas that erupted peralkaline trachyte and phonolite lavas and tuffs from approximately 240 to <10 ka. Suswa is the southernmost volcanic center in the Central Kenya Peralkaline Province (CKPP), a region of intensive geothermal development. This development includes active production at Olkaria and drilling at Menengai as a collaboration between Geothermal Development Company, Ormat, and KenGen. This report focuses on Suswa, which represents the only salic center to have erupted significant volumes of silica-undersaturated lavas and tuffs. The eruptive products of Suswa can be clearly divided into two series, which correspond closely to the volcano's eruptive history. The earlier series (C1) includes lavas and tuffs that built the initial shield volcano and erupted during the first caldera collapse; these rocks are dominated by peralkaline, silica-saturated to mildly under-saturated trachyte. The later series (C2) includes lavas and tuffs that erupted within the caldera structure following the initial collapse and during the creation of a second smaller, nested caldera and central "island block"; these rocks are dominated by peralkaline phonolite. Major-, trace-, and thermodynamic-modelling suggest that C1 is the result of protracted fractional crystallization of a fairly "dry" alkali basalt (<1 wt% H2O) under relatively high pressure (400 MPa) and low oxygen fugacity (FMQ to FMQ-1). Although C1 appears to be primarily the result of closed system processes, a variety of open system processes are responsible for C2. We propose that crystallization of C1 trachyte resulted in the formation of a syenitic residue, which was assimilated during a later stage of recharge and differentiation of alkali basalt to produce post-caldera ne-trachyte. Post-caldera phonolites were in turn the result of fractional crystallization of this ne-trachyte. Later-erupted (ring trench) phonolites, however, are the result of feldspar resorption prompted perhaps by magma recharge as evidenced by reverse zoning in alkali feldspar and linear compatible trace element patterns. This complexity reflects the open-system behavior of East African rift volcanoes, where mafic dikes periodically intrude compositionally evolved shallow magma chambers. Examples of this phenomenon occurred in 2005 in the Afar region of Ethiopia, where an episode of recharge/diking opened a 60 km rupture in the crust, and in 2007, when a magma-driven earthquake swarm struck northern Tanzania for a period of two months and triggered an eruption at Oldoinyo Lengai volcano. Similar recharge is thought to have happened recently at Suswa and a number of the adjacent volcanoes based on geodetic (InSAR).

1. INTRODUCTION

The Central Kenya Peralkaline Province (CKPP) is an area within the Kenyan branch of the East African Rift System (EARS) between approximately 0° and 1.5°S latitude (Fig. 1a; Macdonald and Scaillet, 2006; Macdonald and Bagiński, 2009). The location of the CKPP coincides with the apical region of the Kenya dome, an area of crustal upwarping associated with minor (~1 km) amounts of uplift. The dome is apparently in isostatic equilibrium, being supported by the loading of anomalous mantle within the underlying Lithosphere (Smith, 1994). Salic volcanism in the CKPP has been focused on five centers. These volcanic centers include: (a) two dome fields: the *Eburru Volcanic Complex* composed of trachyte and pantellerite (Omenda, 1997; Velador et al., 2003; Ren et al., 2006), and the *Greater Olkaria Volcanic Complex (GOVC)*, dominated by comendites with minor outcrops of trachyte (Macdonald et al., 1987, 2008a; Clarke et al., 1990; Omenda, 1997; Marshall et al., 2009); and (b) three trachytic caldera volcanoes: *Menengai* with a comenditic to pantelleritic trachyte composition (Leat et al., 1984; Macdonald et al., 2011), *Longonot* composed of pantelleritic trachyte and mixed (trachyte/hawaiite) lavas (Scott and Bailey, 1984; Clarke et al., 1990; Heumann and Davies, 2002; Rogers et al., 2004), and *Suswa*, with trachyte and phonolite lavas and tuffs (Johnson, 1969; Nash et al., 1969; Skilling, 1988, 1993; Scott and Skilling, 1999; White et al., 2012). These shallow volcanic centers all show geothermal manifestations, and, as mentioned in the abstract, are the subject of various stages of production and development. The mafic lava fields Elmenteita, Ndabibi, and Tandamara, lie in the rift floor adjacent to Eburru, Olkaria and Suswa, respectively, and are composed of alkali and transitional basalt, basaltic trachyandesite and trachyandesite.

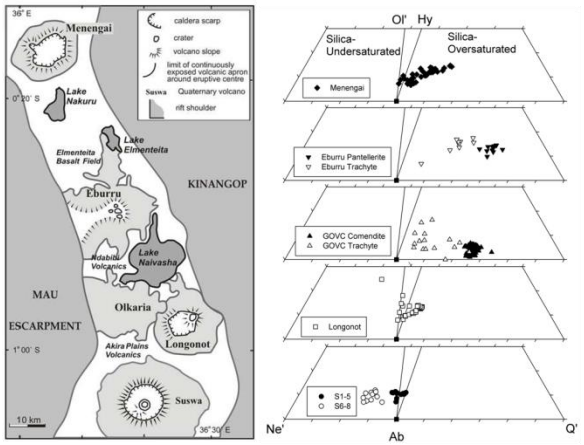

Figure 1: (a) Map of the Central Kenya Peralkaline Province (CKPP; Macdonald and Scaillet, 2006). The subject of this study, Suswa, is the southernmost volcano in the CKPP. (b) Ternary diagram indicating silica saturation for CKPP volcanic centers. Greater Olkaria Volcanic Center (GOVC); S1 – S5 Suswa pre-and syn-caldera units (also referred to as C1 in this paper); S6-S8 Suswa C2 units.

The Suswa volcanic system includes silica-saturated (hypersthene-normative [hy-]trachyte) and silica-undersaturated (nepheline-normative [ne-]trachyte and phonolite) lavas and tuffs, and represents the only salic volcanic system in the CKPP not dominated by silica-oversaturated materials (quartz-normative [q-]trachyte, comendite, and pantellerite) (Fig. 1b). Co-existing oversaturated and undersaturated alkaline igneous suites have also been described from several intra-plate magmatic provinces, including the Massif Central, France (Wilson et al., 1995); the Cameroon line, west Africa (Fitton, 1987); the Marie Byrd Land province, west Antarctica rift system (Panter et al., 1997; LeMasurier et al., 2003, 2011); the Canary Islands (Carracedo et al., 2002); and the Trans-Pecos Magmatic Province, Texas USA (Potter, 1996; White and Urbanczyk, 2001). In each of these provinces, the origin of co-existing silica-oversaturated and undersaturated suites is attributed to either fractional crystallization from a similar alkali basaltic parent with variable degrees of assimilation leading to the formation of two different suites (e.g., Foland et al., 1993), variable degrees of partial melting from a similar asthenospheric source followed by fractional crystallization (e.g., Wilson et al., 1995), or fractional crystallization at differing depths (LeMasurier et al., 2003, 2011). The goal of this study is to model the magma processes that generated the trachyte-phonolite association at Suswa. We propose that fractional crystallization, assimilation, magma mixing, and feldspar resorption played significant roles, with the silica-saturated suite (C1) being primarily the result of protracted fractional crystallization of Ndabibi-like alkali basalt and the silica-undersaturated suite (C2) being primarily the result of coupled assimilation-fractional crystallization from a similar parent (with the syenitic residue from C1 petrogenesis serving as the assimilant) plus feldspar resoprtion triggered by magma recharge. This complexity reflects the open-system behavior of EARS volcanoes, where mafic dikes periodically intrude compositionally evolved shallow magma chambers. Examples of this phenomenon occurred in 2005 in the Afar region of Ethiopia, where an episode of recharge/diking opened a 60 km rupture in the crust (Sigmundsson, 2006; Wright et al., 2006; Yirgu et al., 2006), and in 2007, when a magma-driven earthquake swarm struck northern Tanzania for a period of two months and triggered an eruption at Oldoinyo Lengai volcano (Baer et al., 2008). Similar recharge is thought to have happened at Suswa and a number of the adjacent volcanoes based on geodetic (InSAR) data (Biggs et al., 2009) Modelling also suggests that the silica-undersaturated nature of Suswa may be due to fractional crystallization of alkali basalt at relatively high pressures (~400 MPa) compared to the silica-oversaturated volcanic systems in the CKPP.

2. GEOLOGIC SETTING

The growth of Suswa has been divided into three major stages (Fig. 2; Johnson, 1969; Nash et al., 1969; Skilling, 1988, 1993; Omenda, 1997; Randel and Johnson, 1991). The pre-caldera stage (S1) contains the Pre-caldera Lava Group (PLG), represented by the eruption of dominantly trachytic lavas. The age of this group is presently best estimated by a K-Ar date of 240 ka on "early shield-building lavas" (Baker et al., 1988; Rogers et al., 2004); a preliminary $^{40}Ar/^{39}Ar$ age of ~120 ka has been obtained for lavas exposed in the main caldera wall (A. Deino, personal communication). The syn-caldera stage (S2-5) saw incremental collapse of the caldera roof and eruption of carbonate-rich trachytes through ring fractures to form ignimbrite sheets and trachyte flows, with carbonatite immiscibility in some units (Macdonald et al., 1993). Syn-caldera trachytes contain syenite xenoliths (wall rock). The individual units within the syn-caldera stage include: (a) the Syn-caldera Phreatomagmatic Group (SPG, S2), composed of trachyte pumice lapilli tuffs, basaltic trachyandesitic ash and spatter deposits, and mixed carbonate-trachyte tuffs; (b) the Ring Feeder Group (RFG, S3), including trachytic lava flows; (c) the Western Pumice Group (WPG, S4) consisting of pumice-lapilli tuffs; and (d) the Enkorika Fissure Group (EFG, S5), with trachytic lavas and agglutinate flows (Skilling, 1993). The basaltic trachyandesite ash and spatter in the SPG (S2), which resemble geochemically the mafic flows exposed adjacent to the central volcanoes, are a key aspect of the evidence for periodic magma intrusion and recharge at Suswa. Their presence caused Skilling (1988, 1993) to hypothesize that caldera collapse occurred either by magma-water interaction or introduction of denser trachybasaltic magma into the magmatic chamber.

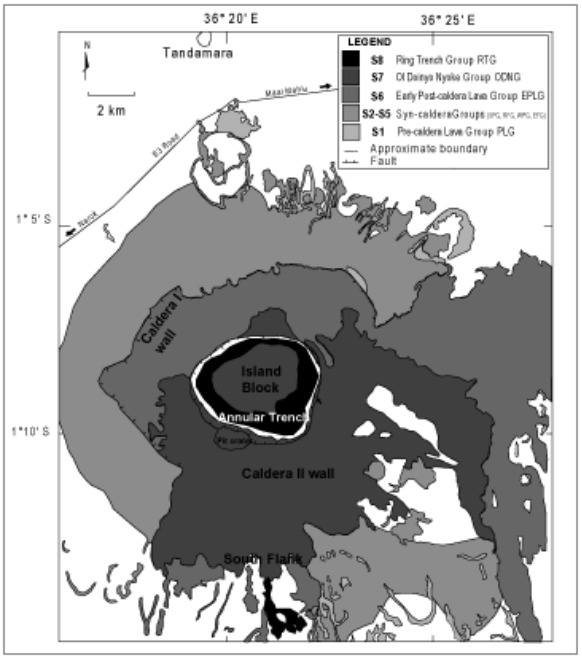

Figure 2: Simplified geologic map of Mount Suswa following Skilling (1988, 1993).

The post-caldera stage (S6-7), erupted from the Ol-Doinyo Nyoke vent on the caldera floor and is divided into two units (Nash et al., 1969; Skilling, 1993; Omenda, 1997): the Early Post-caldera Lava Group (EPLG, S6), which contains aphyric to sparsely phyric trachyte to phonolite lava flows and ash fall deposits; and the Ol-Doinyo Nyoke Group (ODNG, S7), which consists of strongly porphyritic phonolite lava flows. Baker et al. (1988) reported K-Ar ages of 100 ± 10 ka for EPLG (S6) lavas. The eruption of Ol-Doinyo Nyoke was followed by a second caldera collapse and resurgent uplift of the central "island block." Formation of the second caldera and the subsequent uplift led to collapse of a large part of the Ol-Doinyo Nyoke cone, which produced a debris flow deposit (Skilling, 1993). The youngest episode of phonolitic magmatism, the Ring Trench Group (RTG, S8), is associated with the resurgence of the island block in the center of the second caldera and a vent on the southern flank of the volcano (Skilling, 1993). RTG (S8) phonolites are strongly porphyritic, similar to the ODNG (S7) rocks (Omenda, 1997).

Mafic lava fields formed on the rift floor in areas between volcanic complexes. These mafic lavas extruded from fissures and cinder cones, and have basaltic to trachyandesite compositions (Clarke et al., 1990; Omenda, 1997). Elmenteita lava field, located next to Eburru volcanic complex, has porphyritic basalt and basaltic trachyandesite, with plagioclase as the major phenocryst (Clarke et al., 1990; Omenda, 1997). Ndabibi lava field, situated beside the GOVC, has weakly porphyritic basalts with augite and plagioclase as major phenocrysts (Davies and Macdonald, 1987; Omenda, 1997). Tandamara mafic field, adjacent to Suswa in the northern flank, contains basaltic trachyandesite rocks with plagioclase and clinopyroxene as major phenocrysts (Clarke et al., 1990; Omenda, 1997).

3. MINERALOGY AND PETROLOGY

3.1. Silica-Saturated Suite (C1)

3.1.1. Pre-caldera Lava Group (S1)

Pre-caldera Lava Group (PLG) rocks represent the earliest Suswa lavas. These rocks are porphyritic, with dominant alkali feldspar (~25 vol%) and subordinate clinopyroxene and magnetite as the major phyric phases. Accessory minerals include apatite and small olivine grains. The groundmass consists of alkali feldspar, devitrified volcanic glass, rare alkali amphibole, and small vesicles. Alkali feldspar phenocrysts are tabular (2-4 mm), euhedral, and normally zoned from Or_{26} to Or_{36} with low An (<8 mol%). Clinopyroxene crystals are smaller (<0.5 mm) and subhedral with compositions that straddle the join between diopside and hedenbergite ($En_{26-31}Fs_{26-29}Wo_{43-45}$). Magnetite forms small (0.2-0.5 mm), euhedral crystals with a variable composition (Usp_{58-72}). Fluorian (~5 wt% F) apatite occurs as small (30-60 μm), euhedral crystals frequently found in clusters with ferromagnesian minerals. Similar apatite has also been documented in quartz trachytes and rhyolites at the adjacent GOVC (Macdonald et al., 2008b).

3.1.2. Syn-caldera Phreatomagmatic Group (S2)

The Syn-caldera Phreatomagmatic Group (SPG) rocks consist of several trachyte tuffs and minor trachybasalt tephras (Skilling, 1993). Trachytes are porphyritic with alkali feldspar, clinopyroxene, olivine and Fe-Ti oxides as phenocrysts with accessory apatite and fluorite. Trachybasalt tephras consist of clasts of pumice, alkali feldspar, resorbed fragments of broken plagioclase xenocrysts, and syenite xenoliths. Alkali feldspar phenocrysts comprise ~25 vol% of the trachyte tuffs and are smaller than (1-2 mm), but compositionally similar to, crystals in the PLG lavas. One sample of trachyte (KS/94/25) contains alkali feldspars with anorthite contents up to 20 mol% and resorbed xenocrysts of plagioclase ($An_{45-75}Ab_{25-55}$). Clinopyroxene grains are small (~0.5 mm) and euhedral to subhedral, with compositions similar to PLG lavas ($En_{27}Fs_{29}Wo_{44}$). Olivine grains are <0.3 mm and subhedral with compositions about Fa_{76} (White et al., 2012). Magnetite (Usp_{70}) forms small (0.2-0.5 mm), euhedral crystals; in one sample (IS139) a magnetite grain surrounds a few crystals of rutile. Apatite occurs as euhedral to subhedral crystals (up to 80 μm), either as glomerophenocrysts with clinopyroxene, olivine and magnetites or as isolated crystals in groundmass. Alkali amphibole also occurs as a rare, interstitial groundmass phase (Skilling, 1988). Fluorite occurs as small crystals and globules both as a vapor phase filling vesicles and as a primary groundmass phase.

3.1.3. Ring Feeder (S3), Western Pumice (S4), and Enkorika Fissure Groups (S5)

The Ring Feeder Group (RFG) and Enkorika Fissure Group (EFG) are similar units comprised of trachyte lavas; the Western Pumice Group (WPG) consists of aphyric trachyte pumice lapilli tuffs (Skilling, 1993). The phyric assemblage in the RFG and EFG lavas are similar to the PLG lavas, although the alkali feldspar is more Or-rich

($An_{0-3}Ab_{57-60}Or_{40}$). Olivine, clinopyroxene, and magnetite form subhedral to euhedral crystals and occur together as glomerophenocrysts. Clinopyroxene compositions are similar to the PLG ($En_{21-29}Fs_{27-32}Wo_{45-46}$), but olivine is more fayalitic (Fa_{80}). In one sample of the RFG, magnetite composition is Usp_{68}. Rare accessory phases include pyrrhotite in an RFG glomerophenocryst and relatively low-fluorine (~2 wt%) apatite in EFG.

3.2. Silica-Undersaturated Suite (C2)

3.2.1. Early Post-Caldera Lava (S6) and Ol-Doinyo Nyoke (S7) Groups

The post-caldera sequence includes the Early Post-caldera Lava Group (EPLG) and Ol-Doinyo Nyoke Group (ODNG). Both groups consist of geochemically similar phonolites, but differ in terms of their mineralogy: the EPLG is largely aphyric to sparsely phyric, while the ODNG consists of strongly porphyritic phonolite lavas with alkali feldspar, clinopyroxene, olivine, magnetite, and apatite comprising the phyric assemblage. ODNG alkali feldspars consist of zoned anorthoclase crystals ranging in composition from $An_{20}Or_{23}$ to An_5Or_{35} with rims of sanidine (Or_{40-45}). Clinopyroxene, olivine, magnetite, and apatite occur together in these rocks as glomerophenocrysts. Clinopyroxene in these rocks is more magnesian ($Wo_{45-48}Fs_{20-24}En_{30-35}$) than in the pre- and syn-caldera samples. Olivine (Fa_{56-75}) is considerably more abundant in the post-caldera samples compared to the syn-caldera samples, comprising up to 5 vol% of the mode. Fluorian (5-7 wt% F) apatite frequently occurs in melt inclusions in clinopyroxene and olivine from the post-caldera groups, and has a composition similar to groundmass apatite.

3.2.2. Ring Trench Group (S8)

The history of the RTG alkali feldspars is substantially more complex than those of the previous units. Large feldspar phenocrysts (3 – 5 mm) are zoned with euhedral overgrowths surrounding resorbed cores. Feldspar cores have two distinct compositions: (a) high-K cores ($An_{0-5}Ab_{50-60}Or_{30-40}$) similar to pre-caldera feldspars, and (b) low-K cores ($An_{3-15}Ab_{65-70}Or_{15-20}$). Zoning rims have compositional variations between the anorthite (Ca) and orthoclase (K) contents, albite (Na) compositions are constant in all zoned overgrowths. Line scans throughout zoned feldspars confirm the oscillatory composition between cores and overgrowths, and the distinct core composition between different feldspars. Zoned overgrowth compositions overlap those from the cores, although the highest anorthite (An_{20-25}) contents correspond to the overgrowths. The thin rims (~0.01 μm) at the edge of the crystal contain similar composition ($An_{11}Ab_{71}Or_{18}$) to groundmass feldspars (Espejel-Garcia, 2006). A sample (KS/94/01) from the Ring Trench Group contains a melt inclusion inside an alkali feldspar, which also precipitated a small (50μm), euhedral Fe-Ti oxide.

4. WHOLE-ROCK GEOCHEMISTRY

4.1. Classification

Whole-rock samples from Suswa and from mafic volcanic fields in the rift valley, including Elmenteita (White et al., 2012), Ndabibi (Macdonald et al., 2001, 2008a), and Lolonito/Akira/Tandamara (Macdonald et al., 2001, 2008a; White et al., 2012) are classified first with the total alkali-silica (TAS) diagram (Fig. 3a; Le Bas et al., 1986). Silicic samples are further classified as peralkaline (alumina-undersaturated) if their P.I. is ≥1 or if FK/A ≥ 0.60 (White et al., 2003); using these criteria all Suswa trachyte and phonolite samples are peralkaline. The silica-saturation state can only be determined after calculation of a normative mineral assemblage (Fig. 3b): samples with normative quartz (q) and hypersthene (hy) are oversaturated (e.g., quartz- or q-trachyte), samples with normative hy and olivine (ol) are saturated (e.g., trachyte), and samples with normative ol and nepheline (ne) are undersaturated (e.g., nepheline- or ne-trachyte). We use this terminology whether or not quartz or nepheline are present in the modal assemblage. Molecular norms were calculated with a FeO/FeO* ratio of 0.90 for basalt-trachyandesite lavas and 0.85 for trachyte-phonolite lavas (cf. White et al., 2005). These values were determined following the method of Sack et al. (1980) for temperatures between 1200-800°C and oxygen fugacity along the fayalite-magnetite-quartz (FMQ) buffer (Frost et al., 1988). Some mafic to intermediate lavas are generally hy-normative or weakly ne- or q-normative, and may thus be considered "transitional" rather than "alkaline" or "subalkaline" (cf. Barberi et al., 1975). Within the mafic to intermediate suites the samples tend to become silica-oversaturated with increasing differentiation. Pre- and syn-caldera (S1-5) samples classify primarily as peralkaline trachyte and peralkaline ne-trachyte to peralkaline phonolite; post-caldera (S6-7) and Ring Trench Group (S8) samples classify primarily as peralkaline phonolite.

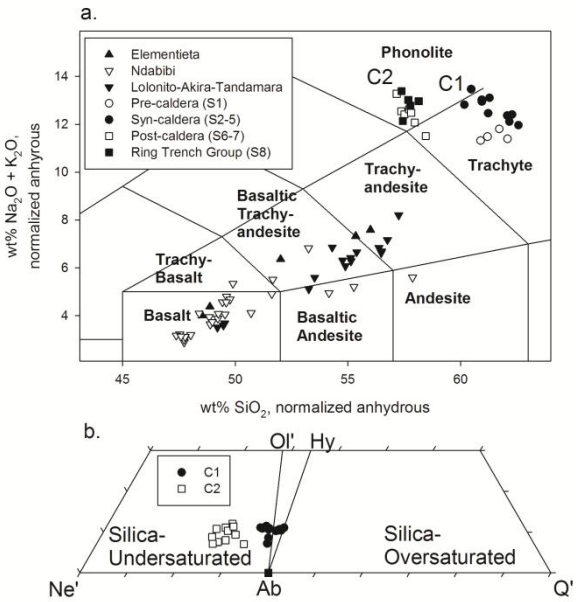

Figure 3: (a) TAS diagram for Suswa and adjacent volcanic fields (basalt through trachyandesite). See Figure 1 for location of adjacent fields. C1: pre- and syn-caldera rocks; C2: post-caldera and Ring Trench Group. (b) Silica saturation diagram for C1 and C2.

4.2. Major-element Geochemistry

SiO_2 is a poor differentiation index for the Suswa rocks - in addition to varying only slightly (~2 wt%) within each

major suite, it tends to decrease with increasing differentiation as measured by indices such as Zr. Therefore, we present major element oxide variation diagrams that use Zr as a differentiation index (Fig. 4). Within increasing Zr, the mafic-intermediate lavas increase in SiO_2, Na_2O, and K_2O, while decreasing in FeO*, MgO, and CaO. Contrasting trends are seen with Al_2O_3 and P_2O_5 concentrations: both decrease with increasing Zr within the Ndabibi suite, while increasing within the Lolonito-Akira-Tandamara suite. Both Suswa suites demonstrate considerable overlap with respect to their Zr concentrations, although most C1 samples have >1000 pm Zr and most C2 samples have <1000 pm Zr. Within both Suswa suites, silica remains fairly constant with increasing Zr, with the C1 suite showing a slight decrease. In both suites, there is a clear negative correlation with respect to Al_2O_3 and a clear positive correlation with respect to FeO*. Also, with increasing Zr, both suites show decreases in MgO, CaO, and P_2O_5, with an increase in Na_2O. As with Al_2O_3, the Ring Trench Group (S8) shows an especially high concentration of Na_2O, especially considering its relatively lower concentration of Zr, which may suggest a role for feldspar accumulation/resorption, volatile enrichment, or both. The behavior of K_2O is strongly decoupled from Na_2O, increasing only slightly with Zr before maintaining a nearly constant (~5 wt%) concentration through both suites.

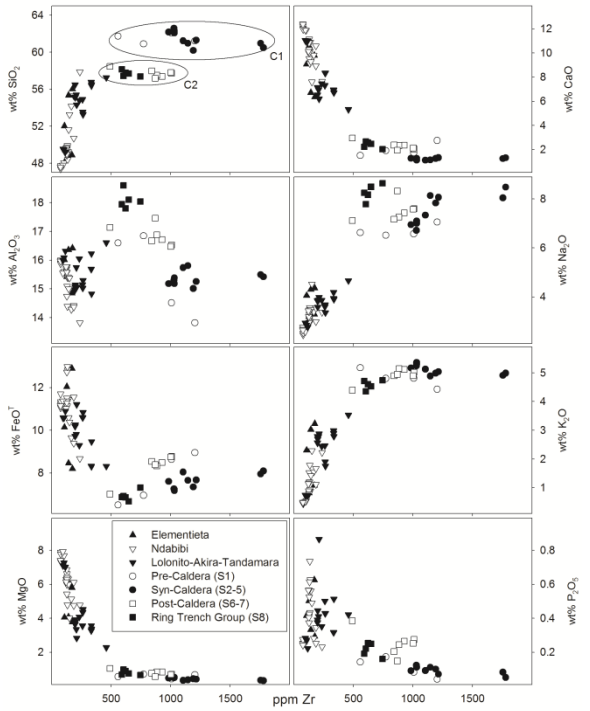

Figure 4: Zr as a differentiation index vs. major and minor elements.

4.3. Trace-element Geochemistry

Variation diagrams that use Zr as a differentiation index plotted against three incompatible trace elements (ITE: Rb, Y, and Nb) and three rare earth element ratios (La_N/Sm_N, Ce_N/Yb_N, and Eu_N/Yb_N; REE normalized following Boynton, 1984) are presented in Fig. 5. All three ITE demonstrate a positive linear correlation with Zr, with variable slopes. Zr/Rb ranges from 2.1 to 8.4 within the mafic suites, with most values around 5.6 (± 1.8). There is no correlation between Zr and Zr/Rb. Average Zr/Rb within the Suswa suites is similar (5.7 ± 1.3); however, unlike the mafic suite there is a clear positive correlation between Zr and Zr/Rb, which increases from 4.2 to 6.4 as Zr increases from 490 to 1200; four samples with >1200 ppm Zr have higher Zr/Rb values (8.0-9.3). Zr/Y values range from 3.4 to 9.8 within the mafic suites. For samples with Zr between 79 and 237 ppm, Zr/Y increases slightly from 3.4 to 5.1; basaltic trachyandesite to trachyandesite samples from Tandamara with higher Zr (>260 ppm) have notably higher Zr/Y (6.2-9.7). Zr/Y values within both Suswa suites are fairly constant (8.4 ± 0.9) and similar to the more evolved samples from Tandamara. There is also a weak positive correlation between Zr and Zr/Nb in the mafic suites, which rises from 3.0 to 5.4 (average 4.0 ± 0.7). Four samples do not follow this trend and have lower (2.6-2.7) values, including three samples from Ndabibi and a single sample of Tandamara basaltic trachyandesite. Zr/Nb ratios from Suswa are fairly constant, and considerably lower than those from the mafic suites (2.5 ± 0.6). The median Zr/Nb ratio in the Suswa suite is 2.2; the average is skewed higher by four samples with Zr/Nb up to 4.0. Scott and Skilling (1999) suggest that these higher-Zr/Nb trachytes may represent batches of Longonot trachyte (Zr/Nb average 4.9) that erupted from the Suswa volcanic center.

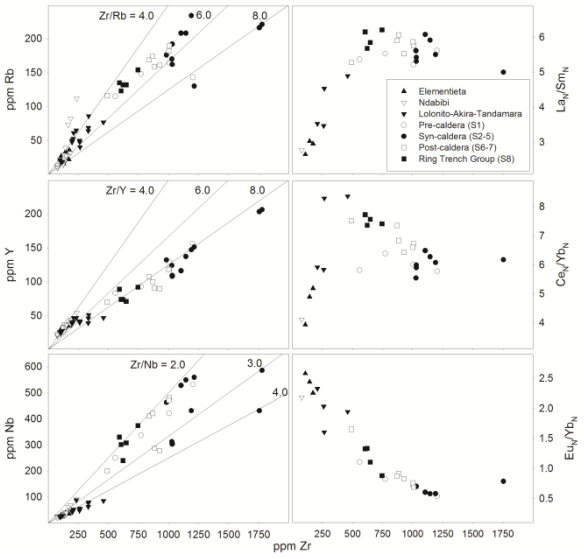

Figure 5: Zr as a differentiation index vs. key trace elements and trace-elemental ratios.

Through all suites, Eu_N/Yb_N decreases with increasing Zr before becoming approximately constant at >1100 ppm Zr, possibly due to the increasingly incompatible behavior of Eu with respect to alkali feldspar as the melt becomes increasingly peralkaline (cf. Mahood and Stimac, 1990; White, 2003; White et al., 2003). Eu_N/Yb_N correlates strongly ($R^2 = 0.93$) with Eu/Eu* (= $Eu_N / \sqrt{[Sm_N \cdot Gd_N]}$ or = $Eu_N / [Tb_N - 2\cdot(Tb_N - Sm_N)/3]$) throughout these suites (not shown). A negative Eu anomaly (Eu/Eu* < 1.00) is indicated by $Eu_N/Yb_N < 1.65$ (Eu/Eu* = $0.5354\cdot[Eu_N/Yb_N]$

+ 0.1094.) Within the mafic suites, La_N/Sm_N increases with Zr from 2.7 to 4.9, but remains fairly constant within the Suswa C1 and C2 suites (5.7 ± 0.3). Ce_N/Yb_N also demonstrates a positive correlation with Zr through the mafic suites, increasing from 3.9 to 8.4. Ce_N/Yb_N is systematically higher in the C2 suite (6.4 – 7.6) than the C1 suite (5.3 – 6.2). Other trace element variation diagrams are not presented; generally, for similar values of Zr and Eu_N/Yb_N, compared to the C1 suite the C2 suite has lower Ce/Y and lower concentrations of Y and HREE, and higher concentrations of K, Ti, P, Rb, Sr, Nb, Ba, and LREE.

5. PETROGENESIS

5.1. Results of Major-element Modelling

Major-element modelling is herein accomplished with both mass balance (e.g., Bryan et al., 1969) and thermodynamic (MELTS; Ghiorso and Sack, 1995; Asimow and Ghiorso, 1998) techniques. Mass balance modelling tests the feasibility of fractional crystallization hypotheses and constrains the relative proportion of the crystallizing phases. MELTS modelling accomplishes the same results, but can also provide constraints on the order of crystallization as well as the conditions under which crystallization occurred (e.g., temperature, pressure, and oxygen fugacity.)

Mafic rocks with low Zr/Nb ratios (<3.1) in or near the CKPP include the most primitive (Mg# > 0.50) alkali and transitional basalts of the Quaternary Ndabibi Formation (Olkaria), lower Pleistocene alkali basalts of the Thiba Formation (east of Aberdare), Miocene nephelinites of the Ngong Formation, and the Miocene Theloi alkali basalts (Macdonald et al., 2001). We consider the Ndabibi basalts more likely than the others to be parental to the Suswa magmas, since they are the nearest in terms of both space and time. A sample of Ndabibi alkali basalt, ND64 (Davies and Macdonald, 1987; Macdonald et al., 2001, 2008a), was selected as the model parent because of its low Zr (76.4 ppm) and Th (1.74 ppm), and relatively high Mg# (mol $Mg/(Mg+Fe^{2+})$ = 0.56, all iron calculated as Fe^{2+}), Ni (42 ppm) and Cr (72 ppm). Mass balance models using similar parental magmas, such as ND154a (Mg# = 0.57, 77 ppm Zr) and ND30 (Mg# = 0.58, 79 ppm Zr), produce results nearly identical to models that use ND64. A sample of pre-caldera ne-trachyte with the lowest Zr (558 ppm) in the C1 suite, KS/94/33, was selected as the model daughter for Stage 1 fractionation (alkali basalt to ne-trachyte); this sample also serves as the model parent for the second stage of magma petrogenesis (compositional variation within the C1 suite), for which the selected model daughter is KS/94/29. A sample of post-caldera phonolite with the lowest Zr (491 ppm) in the C2 suite, KS/94/03, was selected as the model daughter for Stage 3 petrogenesis (alkali basalt to phonolite).

5.1.1. Mass Balance Modelling

All calculations were managed with Microsoft Office Excel 2007. Representative major-element mass balance models that test fractional crystallization hypotheses for the origin of C1 ne-trachyte from alkali basalt or gabbro (Stage 1), C2 phonolite from alkali basalt (Stage 3), and C1 phonolite from ne-trachyte (Stage 2) are presented in White et al. (2012). Mineral analyses used for modelling Stages 1 and 3, except for magnetite and apatite, are from a sample of Ndabibi alkali basalt (ND154a; Macdonald et al., 2008b). The model magnetite composition is stoichiometric $Usp_{55}Mgt_{45}$; the model apatite composition is stoichiometric $Ca_5(PO_4)_3(OH)_2$. Mineral analyses used for modelling compositional variation in Stage 2 are from samples KS/94/33 (alkali feldspar, clinopyroxene, and magnetite) and IS118 (olivine, apatite). All rock and mineral data used for modelling are normalized anhydrous. These major-element models suggest that the origin of and compositional variation within the C1 suite may be the result of first ~93% fractional crystallization (F = 0.07) of an assemblage of 52% plagioclase, 31% clinopyroxene, 9% magnetite, 7% olivine, and 1% apatite from alkali basalt followed by an additional ~61% fractional crystallization (F = 0.39) of an assemblage dominated by alkali feldspar with subordinate clinopyroxene, magnetite, olivine, and apatite, for a total of ~96% crystallization. The sum of the squares of the residuals ($\Box r^2$) for each model are excellent (0.018 and 0.174, respectively). A major-element model for the origin of C2 phonolite from alkali basalt was also calculated. This model suggests that the C2 suite could have a similar origin as the C1 suite (i.e., lays on the same liquid line of descent), but is the result of a slightly smaller degree of fractional crystallization (~91%, or F = 0.09). These hypotheses will be further tested with thermodynamic and trace element modelling.

5.1.2. MELTS Modelling

Magmatic differentiation processes involving solid-liquid equilibria can be thermodynamically modeled through use of the MELTS algorithm (Ghiorso and Sack, 1995; Asimow and Ghiorso, 1998) via the Adiabat_1ph (version 2.0) software package (Smith and Asimow, 2005). For isobaric processes, MELTS computes phase equilibrium relations by minimization of Gibbs energy given a bulk composition, temperature, pressure, and oxygen fugacity. To model fractional crystallization, MELTS first determines the liquidus temperature and liquidus phase for the bulk composition and specified parameters. Mineral phases (except for a very small fraction, 0.01%) are then subtracted, a new liquid composition is calculated, and the temperature is lowered by 5°C. MELTS then calculates a new equilibrium phase assemblage, and the process is repeated until the solidus temperature, or a temperature specified by the user, has been reached.

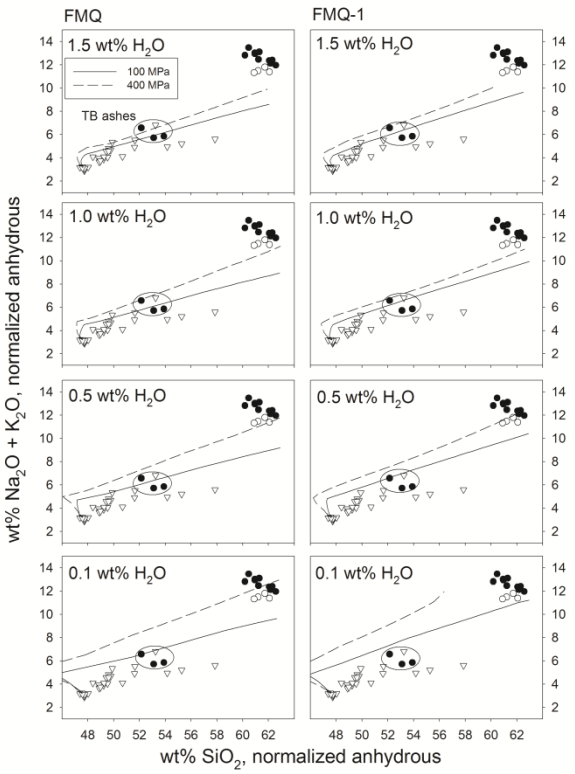

Figure 6: MELTS models for conditions of generation of Suswa samples.

The results of a total of twenty four models of fractional crystallization are presented in Fig. 6. Models variables include two oxygen buffers (FMQ and FMQ-1), four starting water contents (0.1, 0.5, 1.0, and 1.5 wt%), and three pressures of crystallization (100, 400, and 500 MPa). For all models, temperature decreased incrementally from a superliquidus guess of 1400°C. Sample ND64 was selected to represent the composition of the parent or source rock as discussed above. Liquids with a composition similar to KS/94/33 (ne-trachyte) were produced by high-pressure (400 MPa) fractional crystallization models that started with low-H_2O (0.5-1.0 wt%) alkali basalt at low oxygen fugacity (≤FMQ). These models suggest that under these conditions, ne-trachyte may be the result of 82-88% crystallization (F = 0.12-0.18, approximately twice the value predicted by the mass-balance model) of a fractionating assemblage of 35-45% plagioclase, 40-54% clinopyroxene, 5-10% magnetite, 0.6-13% olivine, and 0.4-0.6% apatite from alkali basalt. Higher proportions of plagioclase and lower proportions of clinopyroxene - similar to the results of mass-balance modeling - are associated with crystallization at both lower oxygen fugacities and initial water contents (i.e., 0.5 wt% H_2O and FMQ-1). As one would expect, the relative proportions of magnetite and olivine is solely a function of oxygen fugacity. Generally speaking, lower pressures, higher initial water contents, and higher oxygen fugacities result in less peralkaline, silica-oversaturated melts (q-trachyte) that are the result of a smaller degree of fractional crystallization (F = 0.18-0.29).

5.1.3. Constraints on Pre-eruptive Conditions

The pre-eruptive conditions of the Suswa C1 magma chamber may be constrained by comparing the observed mineral assemblage and whole-rock geochemistry with the results from MELTS, QUIlF, and experiments on phonolitic liquids from literature. Values for intensive thermodynamic parameters for samples of peralkaline trachyte (S1, IS118; S3, 870156) were determined using QUILF95 (Andersen et al., 1993). Calculated clinopyroxene-olivine temperatures range from 858-885°C at a pressure of 100 MPa and from 885-919°C at a pressure of 400 MPa; magnetite compositions in these samples suggest oxygen fugacities between FMQ-0.8 and FMQ-1.1. MELTS results for crystallization at 400 MPa and oxygen fugacity between FMQ and FMQ-1 are consistent with QUIlF geothermobarometic results for S1 and S2 magmas. Additionally, evidence from experimental petrology suggests that the relatively high TiO_2 (>0.60 wt%) in these samples indicate temperatures >890°C (Berndt et al., 2001). Both MELTS and trace element models (which assume $D_{H2O} \approx 0$) suggest that 82-88% fractional crystallization of alkali basalt with an initial concentration of H_2O between 0.5 and 1.0 wt% will result in a slightly water-undersaturated melt (4.1-5.5 wt% H_2O). These high predicted water values are consistent with the presence of alkali amphibole, which occurs as an interstitial groundmass phase in most Suswa lava units and as a common (0.5 to 6.0 vol%) phase in syenite nodules recovered from unit S2 (Skilling, 1988) and the Kilombe volcano (Ridolfi et al., 2006).

Pre-eruptive conditions have been experimentally constrained for several trachytic-phonolitic systems, including the Laacher See volcano (Berndt et al., 2001; Harms et al., 2004), the Kerguelen Archipelago (Freise et al., 2003, 2009), the Canary Islands (Andújar et al., 2008, 2010), and Mount Vesuvius (Scaillet et al., 2008). These studies first indicate that our modelled estimates for pre-eruptive water concentrations are similar to these other systems, which range from ~3 to 6 wt% H_2O. Under these relatively hydrous conditions, amphibole co-exists with sanidine, but only at temperatures lower than those estimated for the Suswa lavas (<815°C; Harms et al., 2004; Scaillet et al., 2008), which may explain the lack of phyric amphibole in the lavas despite its presence in syenites. Experimental results also suggest that the typical phyric assemblage of alkali feldspar + clinopyroxene + magnetite found in Suswa lavas, coupled with the lack of phases such as nepheline, leucite, biotite, and titanite, may further indicate crystallization at relatively high T (>800°C), P (>300 MPa), and H_2O (>4 wt%) (Freise et al., 2003; Scaillet et al., 2008). Such pre-eruptive conditions differ markedly from Vesuvius where, for example, experimental studies have shown that the phonolitic magma chamber has become increasingly shallower with time (Scaillet et al., 2008).

5.1.4. Pearce Element Ratio Diagrams

Pearce (1968) element ratio (PER) diagrams graph ratios of major elements or combinations of major elements with an incompatible element (e.g., Si/Zr, Si+Al/Zr). PER diagrams are based on the stoichiometry of rock-forming

minerals, and slopes of data distributions are equal to major element ratios of minerals lost or gained during differentiation of a cogenetic suite of rocks (Russell and Nicholls, 1988; Stanley and Russell, 1990). For example, data plotted with Si/Zr on the ordinate and Fe/Zr on the abscissa will form a linear trend with a slope that varies depending on the fractionating assemblage from vertical for a phase that lacks stoichiometric Si such as magnetite (Fe_2O_3; Fe:Si = 2/0 = undefined) to horizontal for a phase with non-stoichiometric Fe such as quartz (SiO_2; Fe:Si = 0/1 = 0). PER diagrams for trachtyes and phonolites from Suswa and mafic to intermediate rocks from the nearby Elmenteita, Ndabibi, and Lolonito-Akira-Tandamara volcanic fields (Macdonald et al., 2008a; this report) are presented in Fig. 7.

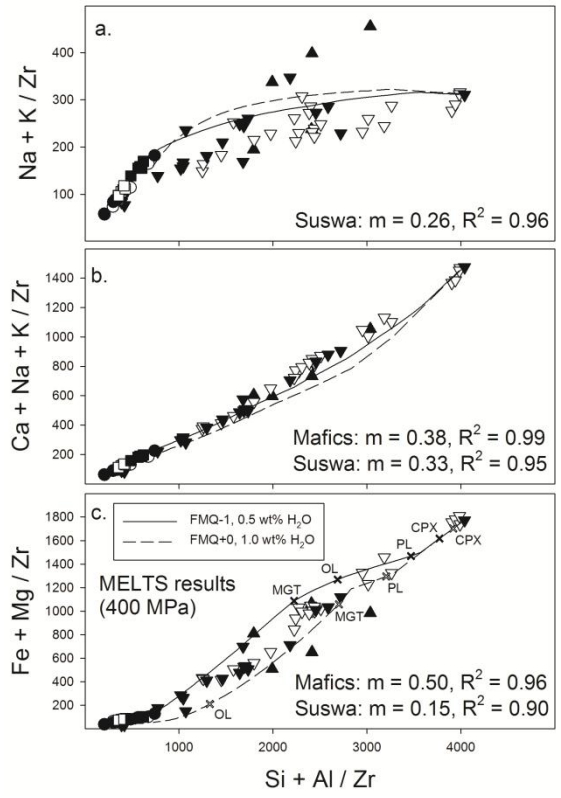

Figure 7: Pearce (1968) element ratio diagrams for Suswa and adjacent fields.

These figures strongly suggest that the mafic to intermediate volcanic fields evolved by similar mechanisms, most probably fractionation of an assemblage dominated by, and with approximately equal amounts of, plagioclase and clinopyroxene. The mathematically predicted slope for clinopyroxene fractionation ([Fe+Mg]:[Si+Al] = 0.50) matches the slope regressed through the data (Fig. 7a), and the average of the predicted slopes for clinopyroxene (Ca:[Si+Al] = 0.50) and plagioclase ([Ca+Na+K]:[Si+Al] = 0.25) is 0.38, which also matches the slope regressed through the data (Fig. 7b). The much lower slope regressed through the alkali data (Fig.7c) is consistent with fractionation of plagioclase with a composition of approximately An_{60}, which is consistent with observed data. Although plots of Ca+Na+K/Zr and Fe+Mg/Zr are consistent with a fractional crystallization origin of the Suswa suite from similar alkali basalts (albeit with a diminished role for clinopyroxene, as suggested by decreased slopes in both plots), the plot of Na+K/Zr precludes fractional crystallization as the sole mechanism responsible for the petrogenesis of Suswa trachyte, since the mafic-intermediate trend intersects the Suswa trend.

Within the Suswa suite, both the C1 and C2 suites follow identical and overlapping trends, which suggest a similar origin and similar processes for within-suite major-element variations. Specifically, the slope regressed through the plot of Na+K/Zr vs. Si+Al/Zr is 0.26, very close to the mathematically predicted slope for alkali feldspar fractionation ([Na+K]:[Si+Al] = 0.25), suggesting that variability of Na and K in the suite is the result of feldspar fractionation, resorption, or accumulation. The slightly higher slope of Ca+Na+K/Zr and smaller slope of Fe+Mg/Zr suggest that clinopyroxene plays a diminished, but still significant role, in the evolution of this suite. These observations accord with the petrography of both the mafic to intermediate centers and the Suswa suite. They are also consistent with the results of MELTS modelling for fractional crystallization of alkali basalt at ~400 MPa pressure, oxygen fugacities between FMQ and FMQ-1, and initial water contents of 0.5-1.0 wt%. For these plots, Zr was estimated from the F-values calculated by MELTS, the concentration of Zr in the parental magma (76.4 ppm), and a bulk partition coefficient for Zr of 0.16 (see below), such that $Zr = 76.4 \cdot F^{-0.84}$.

5.2. Results of trace-element modeling.

5.2.1. Origin of the Pre- and Syn-caldera Suite (S1-5)

Mass-balance and MELTS models suggest that ne-trachyte parental to the C1 suite (represented by sample KS/94/33) may be the result of 93% (mass-balance) or 82-88% (MELTS) fractional crystallization of an assemblage of plagioclase and clinopyroxene with subordinate olivine, magnetite, and apatite from a Ndabibi-like alkali basalt (represented by sample ND64) at relatively high pressure (400 MPa) and low oxygen fugacity (FMQ to FMQ-1). Mass-balance models also suggest that compositional variation within the C1 suite may be further attributed to an additional 60% fractional crystallization of an assemblage dominated by alkali feldspar with subordinate clinopyroxene, olivine, magnetite, and apatite from KS/94/33. These models are further tested with trace-element modelling.

Bulk partition coefficients are calculated for trace element modelling from the results of mass balance modelling and mineral/melt partition coefficients from Caroff et al. (1993) for all minerals except apatite (Fujimaki, 1986) for Stage 1 and mineral/melt partition coefficients from Villemant et al. (1981), Villemant (1988), Mahood and Stimac (1990), White et al. (2003), and Dawson et al. (2008) for Stage 2. Selected bulk partition coefficients for plagioclase and clinopyroxene were also calculated using the formulations of Bindeman et al. (1998) and Wood and Blundy (1997), respectively, with inputs (X_{An}, T for plagioclase; melt chemistry, P, and T for clinopyroxene) derived from MELTS results; in both cases, bulk partition coefficients

were similar for incompatible trace elements, but Sr and Ba were systematically higher for the calculated values compared to the "static" values of Caroff et al. (1986). The results of trace-element modelling of the petrogenesis of alkali basalt to ne-trachyte are presented as spiderdiagrams (Thompson, 1982) in Fig. 8a (ND64 to KS/94/33) and 8b (KS/94/33 to KS/94/29). These results are in agreement with those derived from major-element modelling, suggesting ~90% fractional crystallization for Stage 1 and ~60% fractional crystallization for Stage 2 for a total of ~96% crystallization.

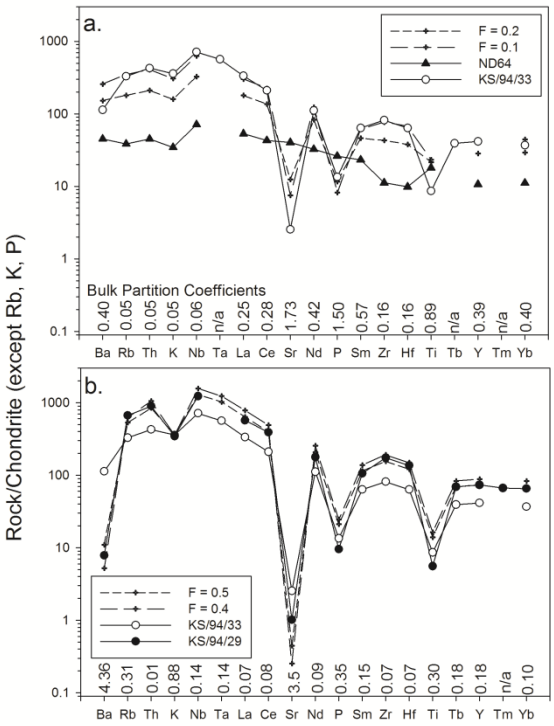

Figure 8: Multi-element variation (following Thompson, 1982). (a) Degree of fractionation required to generate C1 ne-trachyte (KS/94/33) from mafic rock (ND64). F is fraction of melt remaining. Bulk partition coefficients used in modeling are indicated on X-axis. (b) Degree of fractionation required for C1 ne-trachyte to C2 (KS/94/29).

5.2.2. Origin of the Post-caldera Suite (S6-7)

Although mass-balance modelling suggests that ne-trachyte parental to the C2 suite (represented by KS/94/03) may lie on the same liquid line of descent (LLOD) as KS/94/03 as the result of a slighter (~2% less) degree of fractional crystallization, MELTS models indicate no such relationship. This is, of course, consistent with the mineralogical evidence presented above that strongly recommends a role for open-system processes in the petrogenesis of the C2 suite, and especially in the RTG. Additional evidence for this may be provided by trace-element geochemistry, notably the elevated values of LREE/HREE and Ce/Y in the C2 suite compared to the C1 suite. We postulate that the fractional crystallization of C1 ne-trachyte to phonolite would have left behind a syenitic residue similar to xenoliths described from the Kilombe volcano (Ridolfi et al., 2006), and that a later intrusion of alkali basalt (again similar to ND64) may have assimilated this syenitic material during fractional crystallization which resulted in the origin of the C2 suite. This postulation is tested with trace-element models of assimilation and fractional crystallization (DePaolo, 1981) presented in Fig 9. All model parameters (parent, bulk partition coefficients) are identical to those used to model the origin of C1, with an average of "normal" Kilombe syenite analyses taken to represent the assimilant. Assimilation of such a syenite will result in melts with elevated Ce/Y and similar Zr/Nb ratios compared to the C1 suite. The ne-trachyte parental to C2 (KS/94/03) could be the result of 80% crystallization of alkali basalt coupled with a small degree (Ma/Mc = 0.1) of syenite. AFC model results are also presented on a spiderdiagram (Thompson, 1982; Fig. 9), which confirm these results. Lower amounts of fractional crystallization coupled with assimilation of silica-undersaturated syenite would thus result in melts similar to C1, but with lower SiO_2, lower incompatible trace element concentrations, and higher Na_2O, Sr, and Ba as observed. Compositional variation within the C2 suite is the result of both closed- and open-system processes (Fig 10): fractional crystallization of alkali feldspar is responsible for most of the variation within the post-caldera (S6-7) portion of the C2 suite, but mineralogical evidence precludes this from also being true of S8.

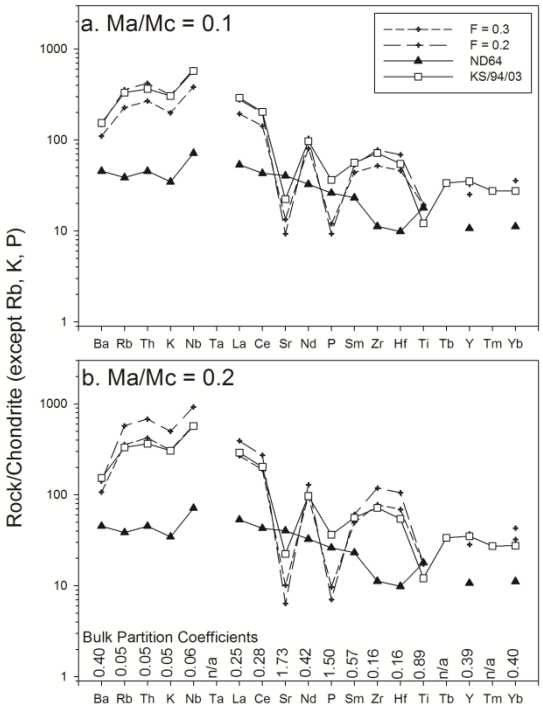

Figure 9: Spiderdiagram (Thompson, 1982) for assimilation/fractional crystallization models.

5.2.3. Origin of the Ring Trench Group (S8)

Mineralogical and trace element data provide compelling evidence for a significant role for magma mixing and feldspar resorption within the Ring Trench Group. Anorthoclase crystals in RTG lavas exhibit both normal and reverse zoning, compatible trace elements concentrations are high compared to the rest of the C2 suite (>190 ppm Sr, >1000 ppm Ba), and trace element diagrams that plot Rb

versus compatible elements (Sr, Ba) form strongly linear trends (Fig. 10). If we postulate from this evidence that compositional variation within these lavas is the result of mixing processes, then it is a relatively trivial exercise to determine the chemical characteristics of the end-members involved in these processes. One likely end-member is represented by sample KS/94/22, one of the more evolved magmas of the post-caldera suite (S6-7). Potential values of Sr, Y, Zr, Nb, and Ba for the other end-member can be constrained by determining the equations of linear regressions of these versus Rb through the RTG samples plus KS/94/22 and then calculating these values over a series of values for Rb calculated for the other end member as a function of proportion of mixing by re-arranging the linear mixing formula to:

$C_2 = (C_H - C_1 + \square C_1) / \square$, (1)

where C_2 is the composition of the hypothetical other end member, C_1 is the composition of the starting magma composition (taken to be KS/94/22), C_H is the composition of hybrid magma (taken to be KS/94/44, the sample of RTG with the lowest Rb, 123 ppm), and $\square$ is the proportion of C_2 relative to C_1.

These results for Sr and Ba are presented in Fig. 10, along with the calculated LLOD for fractional crystallization of the post-caldera (S6-7) suite and the curve for the composition of the corresponding solid residue. All five curves (including those not presented) intersect the solid residue curve at approximately the same point and proportion of mixing; although the curves shown also seem to indicate that one of two samples of Lolonito basalt could also be a potential end-member, this is not suggested by the incompatible elements. Therefore, it seems most likely that compositional variation within the RTG is due to ~45% resorption of an early-crystallized fraction of the feldspar-dominated assemblage previously formed during fractional crystallization of the post-caldera suite or perhaps of the RTG suite prior to resorption. We propose that resorption was driven by thermal disequilibrium: reheating of the RTG magma chamber (which was otherwise evolving along a LLOD similar to the S6-7 suite) due to a likely intrusion of basaltic magma.

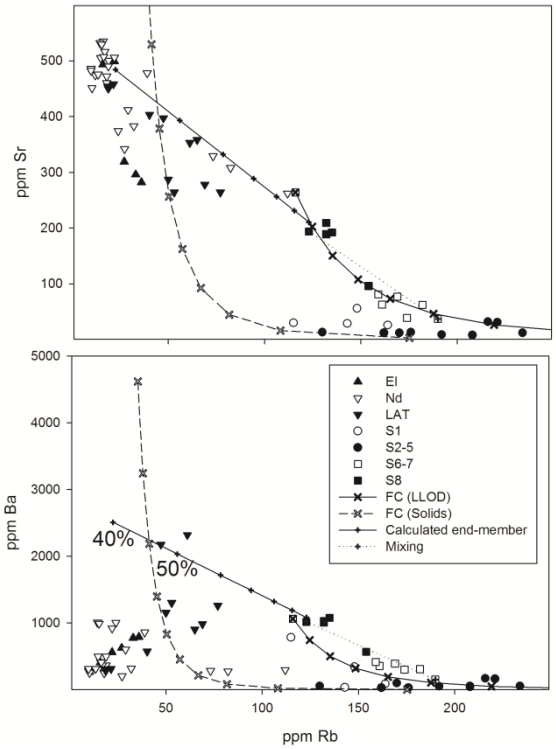

Figure 10: Trace element models for fractional crystallization and mixing in Suswa samples.

6. CONCLUSIONS

1. The initial shield-building trachyte and ne-trachyte lavas (PLG, S1) that built the Suswa volcanic edifice were the result of protracted (90-96%) fractional crystallization of an Ndabibi-like basalt with relatively low initial H_2O concentrations (<1 wt%) under reducing conditions (FMQ-1) at relatively high pressure (400 MPa). This pressure corresponds to a depth of approximately 14km, which corresponds to the boundary between the upper and middle crust in the southern CKPP (Mooney and Christensen, 1994) that may have served as a regional magma trap. This conclusion implies that if Ndabibi basalts are also parental to silica-oversaturated trachytes and rhyolites that comprise the Greater Olkaria volcanic center (Macdonald et al., 2008b; Marshall et al., 2009), then they must have differentiated at a much more shallower level - a conclusion supported by experimental data that suggest that GOVC magma was stored at around 100 MPa (Scaillet and Macdonald, 2001). This is consistent with the mechanism described by LeMesurier et al. (2003, 2011) for co-existing trachyte, rhyolite, and phonolite in the Marie Byrd Land, western Antarctica rift system.

2. Petrogenesis of the syn-caldera units, the eruption of which resulted in the formation of the first Suswa caldera, was clearly similar to the petrogenesis of the pre-caldera lavas as evidenced by identical major- and trace-element concentrations and intra-suite variation. However, the presence of a greater amount of pyroclastic activity, the contemporaneous eruption of trachybasaltic ashes, and the eruption of carbonate-rich trachytes strongly indicates a greater degree of complexity. A detailed study of the syn-caldera units will be necessary to resolve these issues.

3. Fractional crystallization of pre- and syn-caldera trachytes resulted in the formation of a syenitic residue. We propose that recharge of Ndabibi-like basalt into a warm, crystallized or partially crystallized syenitic magma chamber provided a ready assimilant for this basalt. Modelling suggests that a relatively small (Ma/Mc = 0.1) amount of assimilation coupled with a lesser degree (80-90%) of fractional crystallization compared to the earlier suites resulted in the formation of lower-silica, more silica-undersaturated trachyte that characterizes the post-caldera suite.

4. Fractional crystallization of anorthoclase from post-caldera ne-trachyte resulted in the formation of phonolite lavas that built the Ol-Doinyo Nyoke cone. A later injection of basaltic magma appears to have created thermal disequilibrium within the phonolitic magma chamber which resulted in the resorption of these anorthoclase phenocrysts, which is seen in a linear "overprinting" of post-caldera fractional crystallization.

5. Although fractional crystallization was a dominant mechanism in the petrogenesis of the Suswa volcano, open system processes driven by recharge of basaltic magma, including assimilation and feldspar resorption were clearly important processes - especially with respect to the origin of the post-caldera and ring trench groups.

6. Understanding the magmatic processes, such as we have done in this report is important to conceptualizing the development and persistence of the geothermal resource. It also allows us and other researchers to compare and contrast the CKPP with geothermal resources around the world. In this way, geothermal exploration globally is benefitted.

REFERENCES

Andersen, D.J., Lindsley, D.H., and Davidson, P. M.: QUILF: a PASCAL program to asses equilibria among Fe-Mg-Mn-Ti oxides, pyroxenes, olivine, and quartz. *Computers and Geosciences*, **19**, (1993), 1333-1350.

Andújar, J., Costa, F., Martí, J., Wolff, J.A., and Carroll, M.R.: Experimental constraints on pre-eruptive conditions of phonolitic magma from the caldera-forming El Abrigo eruption, Tenerife (Canary Islands). *Chemical Geology*, **257**, (2008), 173-191.

Andújar, J., Costa, F., and Martí, J.: Magma storage conditions of the last eruption of Teide volcano (Canary Islands, Sparin). *Bulletin of Volcanology*, **72**, (2010), 381-395.

Asimov, P.D., and Ghiorso, M. S. Algorithmic modifications extending MELTS to calculate subsolidus phase relations. *American Mineralogist*, **83**, (1998), 1127-1131.

Baer, G., Hamiel, Y., Shamir, G., and Nof, R.:. Evolution of magma-driven earthquake swarm and triggering of the nearby Oldoinyo Lengai eruption, as resolved by InSAR, ground observations and elastic modeling, East African Rift, 2007. *Earth and Planetary Science Letters*, **272**, (2008), 339-352.

Biggs, J., Anthony, E.Y., Ebinger, C.J.: Multiple inflation and deflation events at Kenyan volcanoes, East Africa Rift. *Geology*, **37**, (2009), 979-982.

Bailey, D.K., Macdonald, R.: Fluorine and chlorine in peralkaline liquids and the need for magma generation in an open system. *Mineralogical Magazine*, **40**, (1975), 405-414.

Baker, B.H., Mitchell, J.G., Williams, L.A.J.: Stratigraphy, geochronology and volcano-tectonic evolution of the Kengdon-Naivasha-Kinangop region, Gregory Rift Valley, Kenya. *Journal of the Geological Society of London*, **145**, (1988), 107-116.

Barberi, F., Ferrara, G., Santacroce, R., Treuil, M., Varet, J.: A transitional basalt-pantellerite sequence of fractional crystallization, the Boina Centre (Afar Rift, Ethiopia). *Journal of Petrology*, **16**, (1975), 22-56.

Berndt, J., Holtz, F., Koepke, J.: Experimental constraints on storage conditions in the chemically zoned phonolitic magma chamber of the Laacher See volcano. *Contributions to Mineralogy and Petrology*, **140**, (2001), 469-486.

Bindeman, I.N., Davis, A.M., Drake, M.J.: Ion microprobe study of plagioclase-basalt partition experiments in natural concentration levels of trace elements. *Geochimica et Cosmochimica Acta*, **62**, (1998), 1175-1193.

Boynton, W.R.: Cosmochemistry of the rare earth elements: meteorite studies, Elsevier, Amsterdam, Rare Earth Element Geochemistry. (1984)

Bryan, W.B., Finger, L.W., Chayes, F.: Estimating proportions in petrographic mixing equations by least-squares approximation. *Science*, **163**, (1969), 926-927.

Caroff, M., Maury, R.C., Leterrier, J., Joron, J.L., Cotton, J., Guille, G.: Trace element behavior in the alkali basalt-comenditic trachyte series from Mururoa Atoll, French Polynesia. *Lithos*, **30**, (1993), 1-22.

Carracedo, J.C., Perez Torrado, F.J., Ancochea, E., Meco, J., Hernan, F., Cubas, C.R., Rodriguez-Badiola, E., Ahijado, A.: Cenozoic volcanism II: the Canary Islands. *The Geological Society of London*, **18**, (2002), 439-472.

Clarke, M.C.G., Woodhall, D.G., Allen, D., Darling, G.: Geological, volcanological and hydrogeological controls on the ocurrence of geothermal activity in the area surrounding Lake Naivasha, Kenya, Ministry of Energy, 138 p. (1990)

Davies, G.R., and Macdonald, R.: Crustal influences in the petrogenesis of the Naivasha basalt-comendite complex: combined trace element and Sr-Nd-Pb isotope constraints. *Journal of Petrology*, **28**, (1987), 1009-1031.

Dawson, J.B., Hinton, R.W.: The composition of anorthoclase and nepheline in Mount Kenya phonolite and Kilimanjaro trachyte, and crystal-glass partitioning of elements. *Canadian Mineralogist*, **46**, (2008), 1455-1464.

DePaolo, D.J.: Trace elements and isotopic effects of combined wall rock assimilation and fractional crystallization. *Earth and Planetary Science Letters*, **53**, (1981), 189-202.

Espejel-García, V.V.: Magma dynamics inferred from feldspar zoning in post-caldera phonolites, Suswa volcano, Kenya Rift, Africa. Doctoral Dissertation, University of Texas at El Paso, 175 p. (2006)

Fitton, J.G.: The Cameroon line, west Africa: a comparison between oceanic and continental alkaline volcanism. *The Geological Society of London*, Special publications **30**, (1987) 273-291.

Foland, K.A., Landoll, J.D., Henderson, C.M.B., Chen, J.: Formation of cogenetic quartz and nepheline syenites. *Geochimica et Cosmochimica Acta*, **57**, (1993) 697-704.

Freise, M., Holtz, F., Koepke, J., Scoates, J., Leyrit, H.: Experimental constraints on the storage conditions from the Kerguelen Archipelago. *Contributions to Mineralogy and Petrology*, **145**, (2003) 659-672.

Freise, M., Holtz, F., Nowak, M., Scoates, J.S., Strauss, H.: Differentiation and crystallization conditions of basalts from the Kerguelen large igneous province: an experimental study. *Contributions to Mineralogy and Petrology*, **158**, (2009) 505-527.

Frost, B.R., Lindsley, D.H., Andersen, D J.: Fe-Ti oxide-silicate equilibria assemblages with fayalitic olivine. *American Mineralogist*, **73**, (1988) 727-740.

Fujimaki, H.: Partition coefficients of Hf, Zr, and REE between zircon, apatite and liquid. *Contributions to Mineralogy and Petrology*, **94**, (1986) 42-45.

Ghiorso, M S., Sack, R.O.: Chemical mass transfer in magmatic processes IV. A revised and internally consistent thermodynamic model for the interpolation and extrapolation of liquid-solid equilibria in magmatic systems at elevated temperatures and pressures. *Contributions to Mineralogy and Petrology*, **119**, (1995) 197-212.

Harms, E., Gardner, J.E., Schmincke, H.-U.: Phase equilibria of the lower Laacher See tephra (East Eifel, Germany): constraints on pre-eruptive storage conditions of a phonolitic magma reservoir. *Journal of Volcanology and Geothermal Research*, **134**, (2004) 135-148.

Heumann, A., Davies, G.R.: U-Th disequilibrium and Rb-Sr age constraint on the magmatic evolution of peralkaline rhyolites from Kenya. *Journal of Petrology*, **43**, (2002) 557-577.

Johnson, R. W.: Volcanic geology of Mount Suswa, Kenya. *Philosophical Transactions of the Royal Society of London*, **265**, (1969) 383-412.

Le Bas, M J., Le Maitre, R.W., Streckeisen, A., Zanettin, B.: A chemical classification of volcanic rocks based on the total alkali-silica diagram *Journal of Petrology*, **27**, (1986) 745-750.

Leat, P.T., Macdonald, R., Smith, R.L.: Geochemical evolution of the Menengai Caldera Volcano, Kenya. *Journal of Geophysical Research*, **89**, (1984) 8571-8592.

LeMasurier, W.E., Futa, K., Hole, M., Kawachi, Y.: Polybaric evolution of phonolite, trachyte, and rhyolite volcanoes in eastern Marie Byrd Land, Antarctica: controls on peralkalinity and silica saturation. *International Geology Review*, **45**, (2003) 1055-1099.

LeMasurier, W.E., Choi, S.H., Kawachi, Y., Mukasa, S.B., Rogers, N. W.: Evolution of pantellerite-trachyte-phonolite volcanoes by fractional crystallization of basanite magma in a continental rift setting, Marie Byrd Land, Antarctica. *Contributions to Mineralogy and Petrology*, **162**, (2011), 1175-1199.

Macdonald, R., Baginski, B.: The central Kenya peralkaline province: a unique assemblage of magmatic systems. *Mineralogical Magazine*, **73**, (2009) 1-16.

Macdonald, R., and Scaillet, B.: The Central Kenya Peralkaline Province: insights into the evolution of peralkaline salic magmas. *Lithos*, **91**, (2006) 59-73.

Macdonald, R., Davies, G.R., Bliss, C.M., Leat, P.T., Bailey, D.K., Smith, R.L.: Geochemistry of high-silica peralkaline rhyolites, Naivasha, Kenya Rift Valley. *Journal of Petrology*, **28**, (1987) 979-1008.

Macdonald, R., Kjarsgaard, B.A., Skilling, I.P., Davies, G.R., Hamilton, D.L., Black, S.: Liquid immiscibility between trachyte and carbonate in ash flow tuffs from Kenya. *Contributions to Mineralogy and Petrology*, **114**, (1993) 276-287.

Macdonald, R., Rogers, N.W., Fitton, J.G., Black, S., Smith, M.: Plume-*Lithos*phere interactions in the generation of the basalts of the Kenya Rift, East Africa. *Journal of Petrology*, **42**, (2001) 877-900.

Macdonald, R., Bagiński, B., Belkin, H E., Dzierżanowski, P., Jezak, L.: REE partitioning between apatite and melt in a peralkaline volcanic suite, Kenya Rift Valley. Mineralogical Magazine, **72**, (2008a), 1147-1161.

Macdonald, R., Belkin, H.E., Fiton, J.G., Rogers, N.W., Nejbert, K., Tindle, A G., Marshall, A.S.: The roles of fractional crystallization, magma mixing, crystal mush remobilization and volatile-melt interactions in the genesis of a young basalt-peralkaline rhyolite suite, the Greater Olkaria Volcanic Complex, Kenya rift valley. *Journal of Petrology*, **49**, (2008b), 1515-1547.

Macdonald, R., Bagiński, B., Leat, P.T., White, J.C., Dzierżanowski, P.: Mineral stability in peralkaline silicic rocks: Information from trachytes of the Menengai volcano, Kenya. *Lithos*, **125**, (2011), 553-568.

Mahood, G.A., Stimac, J.A.: Trace-element partitioning in pantellerites and trachytes. *Geochimica et Cosmochimica Acta*, **54**, (1990), 2257-2276.

Marshall, A.S., Macdonald, R., Rogers, N.W., Fitton, J.G., Tindle, A.G., Nejbert, K., Himton, R.W.: Fractionation of peralkaline silicic-magmas: Greater Olkaria volcanic complex, Kenya Rift Valley. *Journal of Petrolog,y* **50**, (2009), 323-359.

Mooney, W.D., Christensen, N.I.: Composition of the crust beneath the Kenya rift. *Tectonophysics*, **236**, (1994), 391-408.

Nash, W.P., Carmichael, I.S.E., Johnson, R.W.: The mineralogy and petrology of Mount Suswa, Kenya. *Journal of Petrology*, **10**, (1969), 409-439.

Noble, D.C.: Sodium, potassium and ferreous iron contents of some secondarily hydrated natural silicic glasses. *American Mineralogist*, **52**, (1967), 280-286.

Omenda, P.A.: The geochemical evolution of Quaternary volcanism in the south-central portion of the Kenya Rift. Doctoral dissertation, University of Texas at El Paso, 218 p. (1997)

Panter, K.S., Kyle, P.R., Smellie, J.L.: Petrogenesis of a phonolite-trachyte succession at Mount Sidley, Marie Byrd Land, Antarctica. *Journal of Petrology* **38**, (1997), 1225-1253.

Pearce, T.H.: A contribution to the theory of variation diagrams. *Contributions to Mineralogy and Petrology* **19**, (1968), 142-157.

Potter, L.S.: Chemical variation along strike in feldespathoidal rocks of the eastern alkalic belt, Trans-Pecos Magmatic Province, Texas and New Mexico. The *Canadian Mineralogist*, **34**, (1996), 241-264.

Randel, R.P., Johnson, R.W.: Geology of the Suswa area, Mines and Geological Department (Nairobi), 41 p. (1991)

Ren, M., Anthony, E.Y., Omenda, P.A., White, J.C., Macdonald, R., Bailey, D.K.: Application of the QUILF thermobarometer to the peralkaline trachytes and pantellerites of the Eburru Volcanic Complex, East African Rift, Kenya. *Lithos*, **91**, (2006), 09-124.

Ridolfi, M., Renzulli, A., Macdonald, R., Upton, B.G.: Peralkaline syenite autoliths from Kilombe volcano, Kenya Rift Valley: evidence for subvolcanic interaction with carbonitic fluids. *Lithos*, **91**, (2006), 373-392.

Rogers, N.W., Evans, P.J., Blake, S., Scott, S.C., Hawkesworth, C.J.: Rates and timescales of fractional crystallization from 238U-230Th-226Ra disequilibria in trachyte lavas from Longonot Volcano, Kenya. *Journal of Petrology*, **45**, (2004), 1747-1776.

Russell, J.K., Nicholls, J.: Analysis of petrologic hypothesis with Pearce element ratios. *Contributions to Mineralogy and Petrology*, **99**, (1988), 25-35.

Sack, R.O., Carmichael, I.S.E., Rivers, M., Ghiorso, M.S.: Ferric-ferrous equilibria in natural silicate liquids at 1 bar. *Contributions to Mineralogy and Petrology*, **75**, (1980), 369-376.

Scaillet, B., Macdonald, R.: Phase relations of peralkaline silicic magmas and petrogenetic implications. *Journal of Petrology*, **42**, (2001), 825-845.

Scaillet, B., Pichavant, M., Cioni, R.: Upward migration of Vesuvius magma chamber over the past 20,000 years. *Nature*, **455**, (2008), 216-220.

Scott, S.C., Bailey, D.K.: Coeruption of contrasting magmas and temporal variations in magma chemistry at Longonot volcano, Central Kenya. *Bulletin of Volcanology*, **47**, (1984), 849-873.

Scott, S.C., Skilling, I.P.: The role of tephrachronology in recognizing synchronous caldera-forming events at the Quaternary volcanoes Longonot and Suswa,south Kenya Rift. *The Geological Society of London*, Special publications, **161**, (1999), 47-67.

Sigmundsson, F.: Magma does the splits. *Nature*, **442**, (2006), 251-252.

Skilling, I. P.: The geological evolution of Suswa Volcano, Kenya. Doctoral dissertation, University of Lancaster. (1988)

Skilling, I.P.: Incremental caldera collapse of Suswa volcano, Gregory rift Valley, Kenya. *Journal of the Geological Society of London*, **150**, (1993), 885-896.

Smith, M.: Stratigraphic and structural constraints on mechanisms of active rifting in the Gregory Rift, Kenya. *Tectonophysics*, **236**, (1994), 3-22.

Smith, P.M., Asimow, P.D.: Adiabat_1ph: A new public front-end to the MELTS, pMELTS, and pHMELTS models. *Geochemistry Geophysics Geosystems*, **6** art. No. Q02004. (2005)

Stanley, C.R., Russell, J.K.: Matrix methods for the development of Pearce element ratio diagrams, Theory and application of Pearce element ratios to geochemical data analysis. Vancouver, Canada, Geological Association of Canada Annual Meeting, (1990), 1311-1156.

Thompson, R.N.: Magmatism of the British Tertiary volcanic province. *Scottish Journal of Geology*, **18**, (1982), 49-107.

Velador, J.M., Omenda, P.A., Anthony, E.Y.: An integrated mapping and remote sensing investigation of the structural control for fumarole location in the Eburru Volcanic Complex, Kenya Rift. *Geothermal Resources Council Transaction,s* **27**, (2003), 639-642.

Villemant, B.: Trace element evolution in the Phlegrean fields (Central Italy): fractional crystallization and selective enrichment. *Contributions to Mineralogy and Petrology*, **98**, (1988), 169-183.

Villemant, B., Jaffrezic, H., Joron, J.L., Treuil, M.: Distribution coefficients of major and trace elements; fractional crystallization in the alkali basalt series of Chaine des Puys (Massif Central, France). *Geochimica et Cosmochimica Acta*, **45**, (1981), 1997-2016.

White, J.C.: Trace-element partitioning between alkali feldspar and peralkalic quartz trachyte to rhyolite magma. Part II: Empirical equations for calculating trace-element partition coefficients of large-ion lithophile, high field-strength, and rare-earth elements *American Mineralogist*, **88**, (2003), 330-337.

White, J.C., Urbanczyk, K.M.: Origins of a silica-oversaturated quartz trachyte-ryolite suite through combined crustal melting, magma mixing, and fractional crystallization: the Leyva Canyon volcano, Trans-Pecos Magmatic Province, Texas. *Journal of Volcanology and Geothermal Research*, **111**, (2001), 155-182.

White, J.C., Holt, G.S., Parker, D.F., Ren,M.: Trace-element partitioning between alkali feldspar and peralkalic quartz trachyte to rhyolite magma. Part I: Systematics of trace-element partitioning. *American Mineralogist*, **88**, (2003), (1995), 316-329.

White, J.C., Ren, M., Parker, D.F.: Variation in mineralogy, temperature, and oxygen fugacity in a suite of strongly peralkaline lavas and tuffs, Pantelleria, Italy. *Canadian Mineralogist*, **43**, (2005), 1331-1347.

White, J.C., Espejel-García, V.V., Anthony, E.Y., Omenda, P.A.: Open system evolution of peralkaline trachyte and phonolite from the Suswa volcano, Kenya Rift. *Lithos*, (2012), doi: 10.1016/j.*Lithos*/2012.01.023.

Wilson, M., Downes, H., Cebria, J.M.: contrasting fractionation trends in coexisting continental alkaline magma series; Cantal, Massif Central, France. *Journal of Petrology*, **36**, (1995), 1729-1753.

Wood, B J., Blundy, J.D.: A predictive model for rare earth element partitioning between clinopyroxene and anhydrous silicate melt. *Contributions to Mineralogy and Petrology*, **129**, (1997), 166-181.

Wright, T.J., Ebinger, C., Biggs, J., Ayele, A., Yirgu, G., Keir, D., Stork, A.: Magma-maintained rift segmentation at continental rupture in the 2005 Afar dyking episode. *Nature*, **442**, (2006), 291-294.

Yirgu, G., Ayele, A., Ayalew, D.: Recent seismovolcanic crisis in Northern Afar, Ethiopia. *Eos Transactions AGU*, **87** (33), (2006), 325-336.